ORNL-TM-4380

cy.1

INFLUENCE OF AGING ON THE IMPACT PROPERTIES OF HASTELLOY N, HAYNES ALLOY NO. 25, AND HAYNES ALLOY NO. 188

H. E. McCoy

D. T. Bourgette

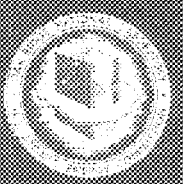

OAK RIDGE NATIONAL LABORATORY

OPERATED BY UNION CARBIDE CORPORATION • FOR THE U.S. ATOMIC ENERGY COMMISSION

ORNL-TM-4380

Contract No. W-7405-eng-26

METALS AND CERAMICS DIVISION

INFLUENCE OF AGING ON THE IMPACT PROPERTIES OF HASTELLOY N, HAYNES ALLOY NO. 25, AND HAYNES ALLOY NO. 188

H. E. McCoy and D. T. Bourgette

DECEMBER 1973

OAK RIDGE NATIONAL LABORATORY
Oak Ridge, Tennessee 37830
operated by
UNION CARBIDE CORPORATION
for the
U.S. ATOMIC ENERGY COMMISSION

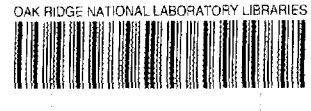

CONTENTS

INFLUENCE OF AGING ON THE IMPACT PROPERTIES OF HASTELLOY N, HAYNES ALLOY NO. 25, AND HAYNES ALLOY NO. 188

H. E. McCoy and D. T. Bourgette

ABSTRACT

Samples of Hastelloy N and Haynes alloy Nos. 25 and 188 were solution annealed, aged at temperatures over the range 650 to 900°C, and impact tested at 25 and 300°C. The impact energy decreased for most aging conditions, with the property changes being least for Hastelloy N and greatest for Haynes alloy No. 25. Small aged tensile samples showed that aging reduced the fracture strain at 25°C. The fractures of the tensile samples were examined, and some of the notched impact specimens were viewed optically. The reduction in toughness of Hastelloy N correlated well with the amount of grain boundary precipitate. Haynes alloys Nos. 25 and 188 formed carbides and Laves phase. These alloys had a strong tendency to fracture intergranularly even in the solution-annealed condition. The tendency increased with aging, and the increased amounts of grain boundary precipitate likely account for the reduction in toughness.

INTRODUCTION

Hastelloy N is a solution-strengthened nickel-base alloy that was developed for good strength and corrosion resistance at about 650°C. No intermetallic compounds have been identified in this alloy, but carbides precipitate and cause modest changes in the properties.[1,2] Haynes alloys Nos. 25 and 188 are cobalt-base alloys that are solid solution strengthened and suitable for use at temperatures up to 1000°C. These cobalt-base alloys experience some property changes due to carbide precipitation, but the formation of brittle Laves phases of the A_2B type is the main cause of embrittlement.[3-5]

Generally, neither the carbides nor the Laves phases cause drastic embrittlement at elevated temperatures, but their effect increases as the temperature is decreased. The degree of embrittlement is also increased by increasing strain rate and by notches and other discontinuities that magnify the average stress. One of the applications that would subject the structural material to impact loading at low temperatures is in isotope power supplies intended for use in space. The material would be aged for several thousand hours at an elevated service temperature, cooled gradually while still in orbit or during reentry, and possibly exposed to impact loading during reentry. Thus, the impact properties after aging are of major concern in this application.

Although the experimental program described in this report was undertaken to provide necessary information for the design of isotope power supplies, numerous other applications require a knowledge of the impact properties of these alloys after prolonged aging. Our specific program involved aging samples of Hastelloy N, Haynes alloy No. 25, and Haynes alloy No. 188 up to 4000 hr at temperatures from 650 to 900°C and measuring their impact properties at 25 and 300°C. Budgetary limitations prohibited detailed phase identification, and only limited metallographic examination was possible.

EXPERIMENTAL DETAILS

Experimental material of the three alloys was obtained in the form of 1/2-in.-thick plate. The vendor's and ORNL's chemical analyses are given in Table 1. The Hastelloy N was double vacuum melted and the Haynes alloys Nos. 25 and 188 were air melted and vacuum arc remelted.

Standard Charpy V-notch impact specimens were machined in conformance with the specifications in ASTM Standard E 23-66. The samples were solution annealed 1 hr at 1150°C in argon and cooled rapidly to ambient temperature. They were wrapped in nickel foil and sealed in quartz in argon at 0.33 atm and aged at various temperatures. Following aging they were broken from the capsule and impact tested at 25 and 300°C according to ASTM Standard E 23-66.

IMPACT DATA

The results of impact tests on Hastelloy N at 25°C are shown in Fig. 1. The material was quite tough in the solution-annealed condition, with an impact energy of 164 ft-lb. Aging at 650 and 700°C caused a gradual decrease in the impact energy to values of 75 and 95 ft-lb, respectively, and then the impact energy increased with further aging. Aging at 900°C resulted in a steady decrease to about 30 ft-lb after aging 4000 hr. Aging at 800°C had little effect for 500 hr, but longer aging resulted in a rapid decrease in the impact energy to a value of 40 ft-lb after aging 4000 hr.

The impact results shown in Fig. 2 for Hastelloy N tested at 300°C are qualitatively similar to those shown in Fig. 1 for 25°C. The impact energies were higher at 300°C, with a value of 235 ft-lb for the solution-annealed material and a minimum value of 70 ft-lb for samples aged at 900°C.

The fractures of the Hastelloy N impact specimens are shown in Fig. 3. The lower smooth part of each sample is the machined portion of the notch. The appearance of the fracture is a qualitative measure of the toughness, with terms of "granular" (brittle) and "fibrous" (ductile) used commonly in the literature. All the samples had fibrous fractures, and three of the samples tested at 300°C had sufficient toughness not to part. The width of the sample at the base of the notch is another measure of plasticity. As the sample deforms longitudinally, it must contract laterally. Thus, the greater the reduction in width at the base of the notch, the greater the toughness. All the samples contracted

Table 1. Chemical Analyses of Alloys

Element	Contents, wt %					
	Hastelloy N[a]		Haynes[b] Alloy No. 25		Haynes Alloy No. 188[c]	
	Vendor	ORNL	Vendor	ORNL	Vendor	ORNL
Cr	7.1	7.0	19.8	18.1	22.7	20.3
Fe	0.47		2.4	2.6	1.6	1.6
Ni	Bal	75.6	10.0	9.5	21.1	21.4
Co	0.08		Bal	52.1	Bal	39.5
Mo	16.7	15.7		0.57		0.39
W		0.03	14.5	13.3	14.1	15.3
C	0.052	0.051	0.12	0.12	0.09	0.11
Si	0.02	0.05	0.08	0.23	0.14	0.33
Mn	0.02	0.02	1.3	1.2	0.81	0.69
Ti	0.06	0.05		<0.01		0.01
Al	0.13	0.2		0.1		0.1
Cu	0.02	0.02		0.03		0.03
P	0.004	0.0020	0.020	0.120	0.009	0.011
S	0.006	0.0020	0.009	0.003	0.001	0.001
B	0.001	0.0020		0.0050		0.0005
La					0.07	0.07

[a]Procured as arc-melted plate 48 × 24 × 1/2 in. from Allvac Metals, heat 6960.

[b]Procured as hot-rolled, pickled, and annealed plate 36 × 76 × 1/2 in. from Stellite Division, Union Carbide Corporation, heat 1860-6-1813.

[c]Procured as plate 30 × 12 × 1/2 in. from Stellite Division, Union Carbide Corporation, heat 1880-8-0132.

appreciably at the base of the notch, but the samples aged at 900°C (rows 2 and 4) showed progressively less reduction in width with increasing aging time.

The variation of impact energy at 25°C with aging time is shown in Fig. 4 for Haynes alloy No. 25 aged at various temperatures. The impact energy in the solution-annealed condition was 70 ft-lb, compared with 164 ft-lb (Fig. 1) for Hastelloy N. Aging at 650, 700, 800, and 900°C caused a progressive decrease in impact energy with aging time, and the

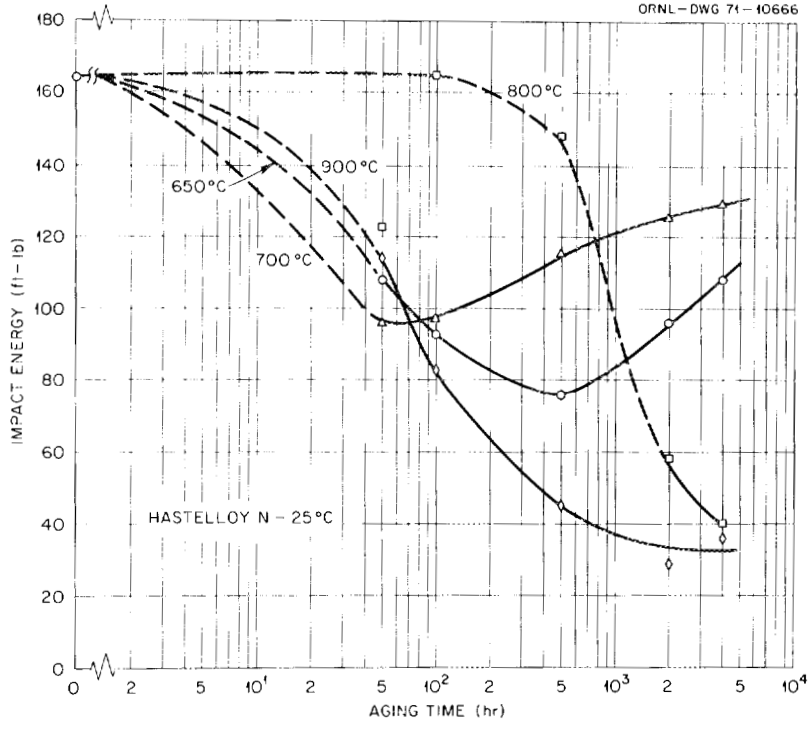

Fig. 1. Variation of Notch-Impact Energy at 25°C With Aging Time for Hastelloy N. Samples annealed 1 hr at 1150°C before aging.

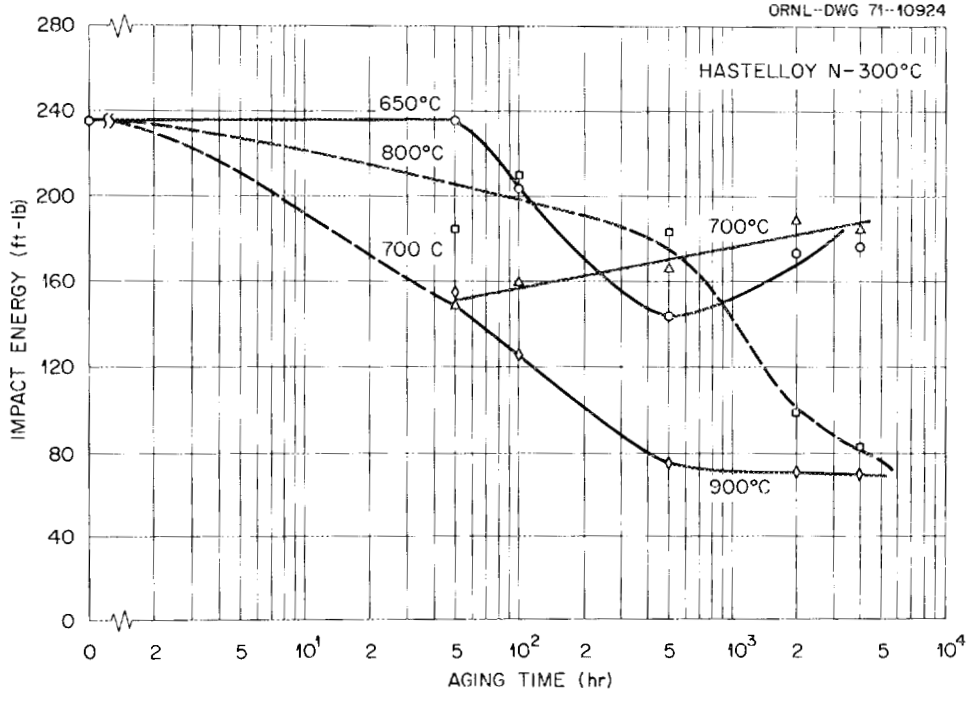

Fig. 2. Variation of Notch-Impact Energy at 300°C With Aging Time for Hastelloy N. Samples annealed 1 hr at 1150°C before aging.

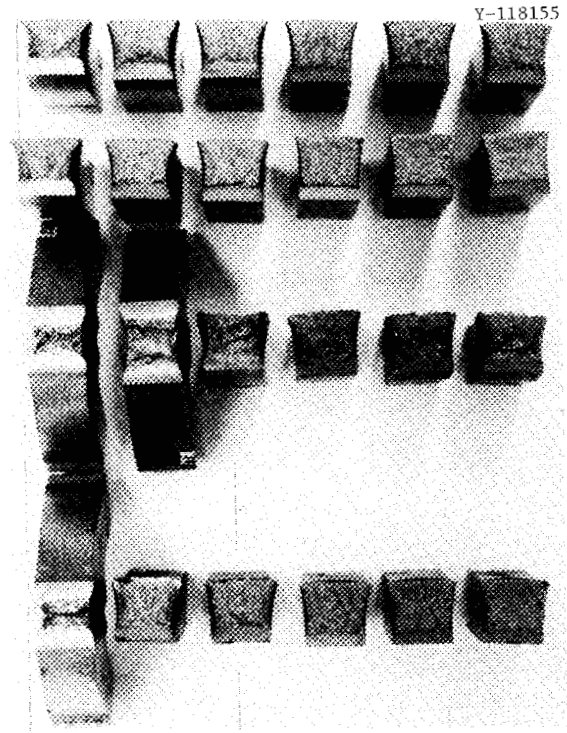

Fig. 3. Fracture Surfaces of Hastelloy N Impact Samples. The aging time increases in each row from zero on the left to 4000 hr on the right. The samples in the top row were aged at 650°C and tested at 25°C, those in the second row were aged at 900°C and tested at 25°C, those in the third row were aged at 650°C and tested at 300°C, and those in the bottom row were aged at 900°C and tested at 300°C.

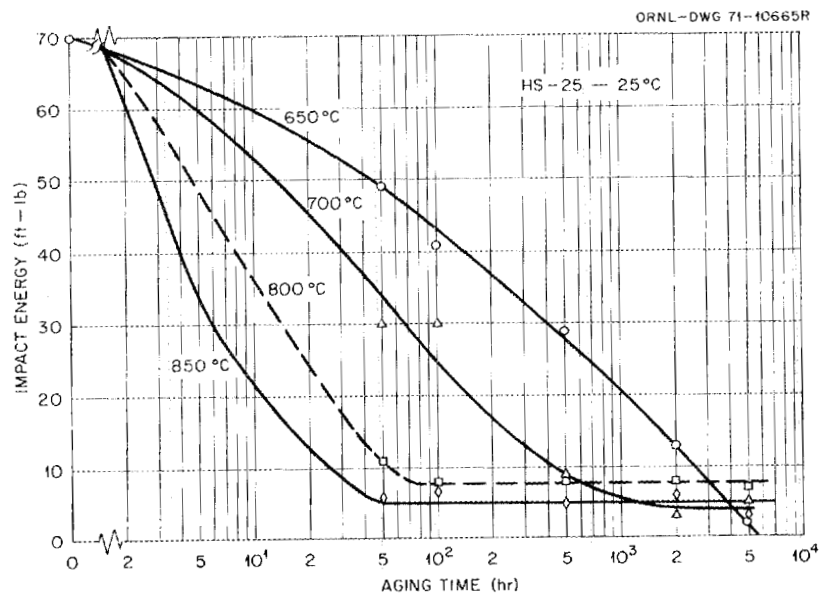

Fig. 4. Variation of Notch-Impact Energy at 25°C With Aging Time for Haynes Alloy No. 25. Samples annealed 1 hr at 1150°C before aging.

rate of decrease increased with increasing aging temperature. The lowest impact energies resulting from aging were from 3 to 8 ft-lb.

The effects of aging on the impact energy of Haynes alloy No. 25 at 300°C are shown in Fig. 5 and are qualitatively similar to the effects noted at 25°C (Fig. 4). The lowest value noted at a test temperature of 300°C was 5 ft-lb for a sample aged at 650°C.

The fracture surfaces in Fig. 6 also reflect the large effect of aging on the impact properties. The top row was aged at 650°C and tested at 25°C. The fracture appearance changed from fibrous to granular, and the reduction in width at the base of the notch decreased with increasing aging time. The second row was aged at 850°C and tested at 25°C; the fracture appearance and the reduction in width indicate a high rate of embrittlement during aging at 850°C. The samples in the third and fourth rows were aged at 650 and 850°C, respectively, and tested at 300°C. They reflect progressive embrittlement with increasing aging time.

The variation of impact energy at 25°C of Haynes alloy No. 188 with aging time is shown in Fig. 7. The impact energy in the solution-annealed condition was 58 ft-lb, compared with 70 ft-lb for Haynes alloy No. 25 and 164 ft-lb for Hastelloy N. Aging at 650°C gradually reduced the impact energy except for a possible increase after aging for 50 hr. Aging at 700°C reduced the impact energy for the first 500 hr, and further aging caused a slight improvement. Aging at 800 and 900°C reduced the impact energy to values of 9 and 6 ft-lb, respectively. The crossover

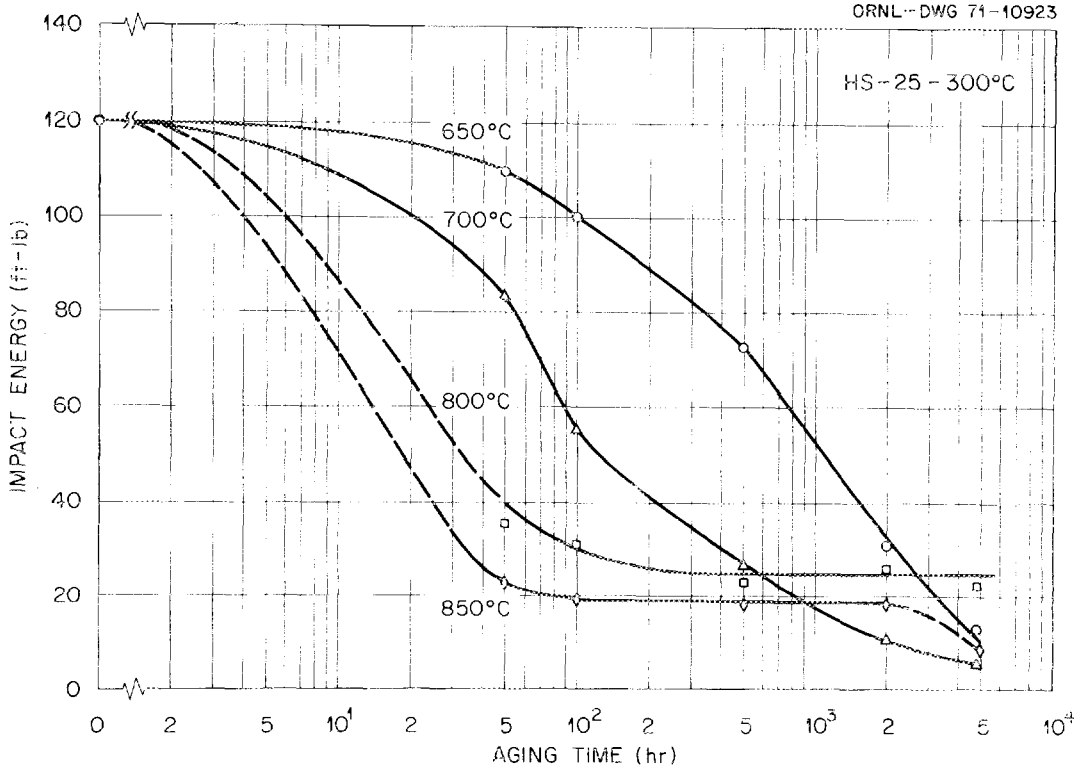

Fig. 5. Variation of Notch-Impact Energy at 300°C With Aging Time for Haynes Alloy No. 25. Samples annealed 1 hr at 1150°C before aging.

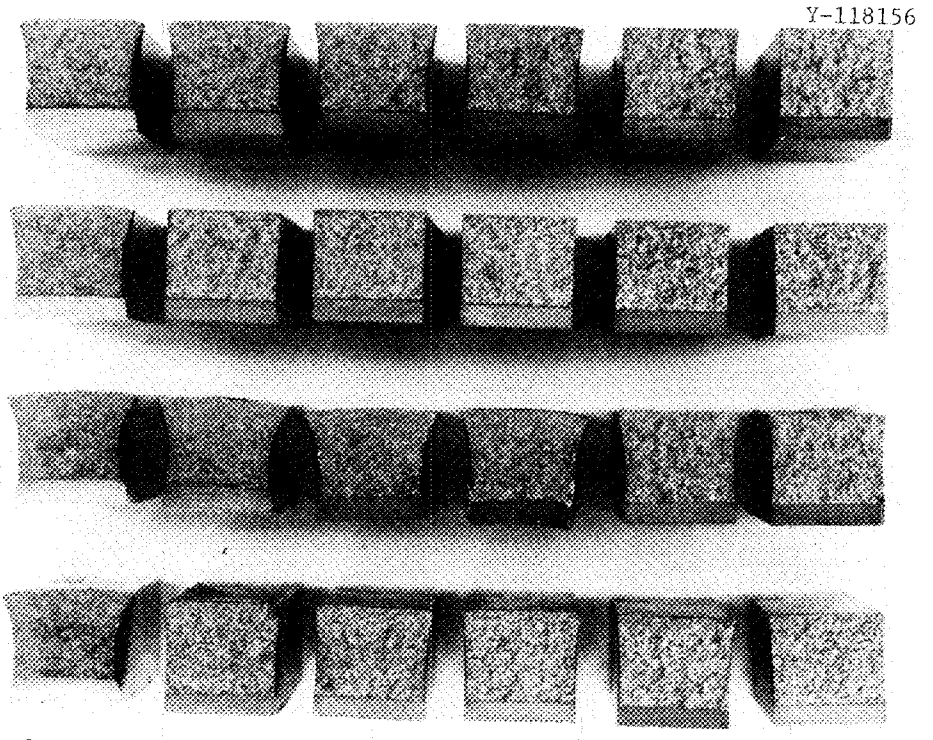

Fig. 6. Fracture Surfaces of Haynes Alloy No. 25 Impact Samples. The aging time increases in each row from zero on the left to 4800 hr on the right. The samples in the top row were aged at 650°C and tested at 25°C, those in the second row were aged at 850°C and tested at 25°C, those in the third row were aged at 650°C and tested at 300°C, and those in the bottom row were aged at 850°C and tested at 300°C.

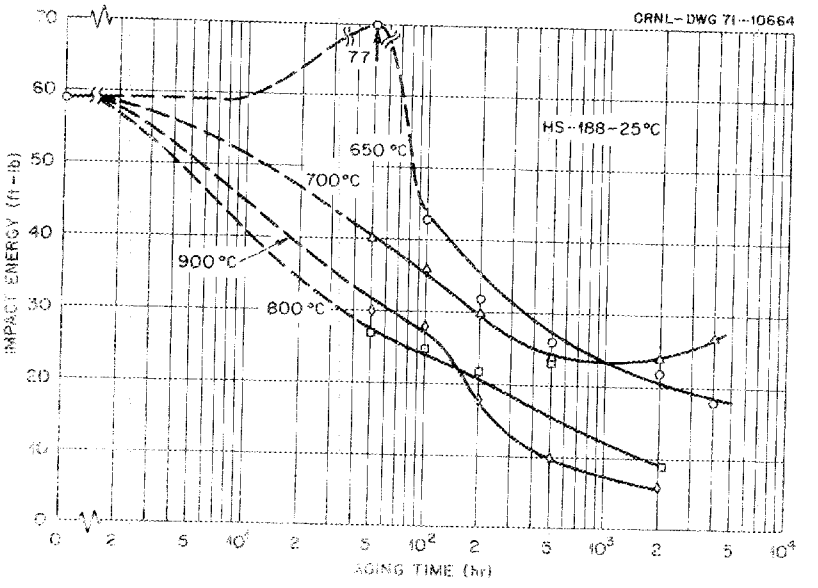

Fig. 7. Variation of Notch-Impact Energy at 25°C With Aging Time for Haynes Alloy No. 188. Samples annealed 1 hr at 1150°C before aging.

in properties for aging temperatures of 800 and 900°C is likely real since the same effect was noted at a test temperature of 300°C (Fig. 8).

The impact results at a test temperature of 300°C for Haynes alloy No. 188 are shown in Fig. 8. These data show the improvement in impact properties after aging 50 hr at 650°C and the crossover in properties after aging at 800 and 900°C. Generally, the data show a gradual decrease in impact energy with aging time and larger effects with increasing aging temperature.

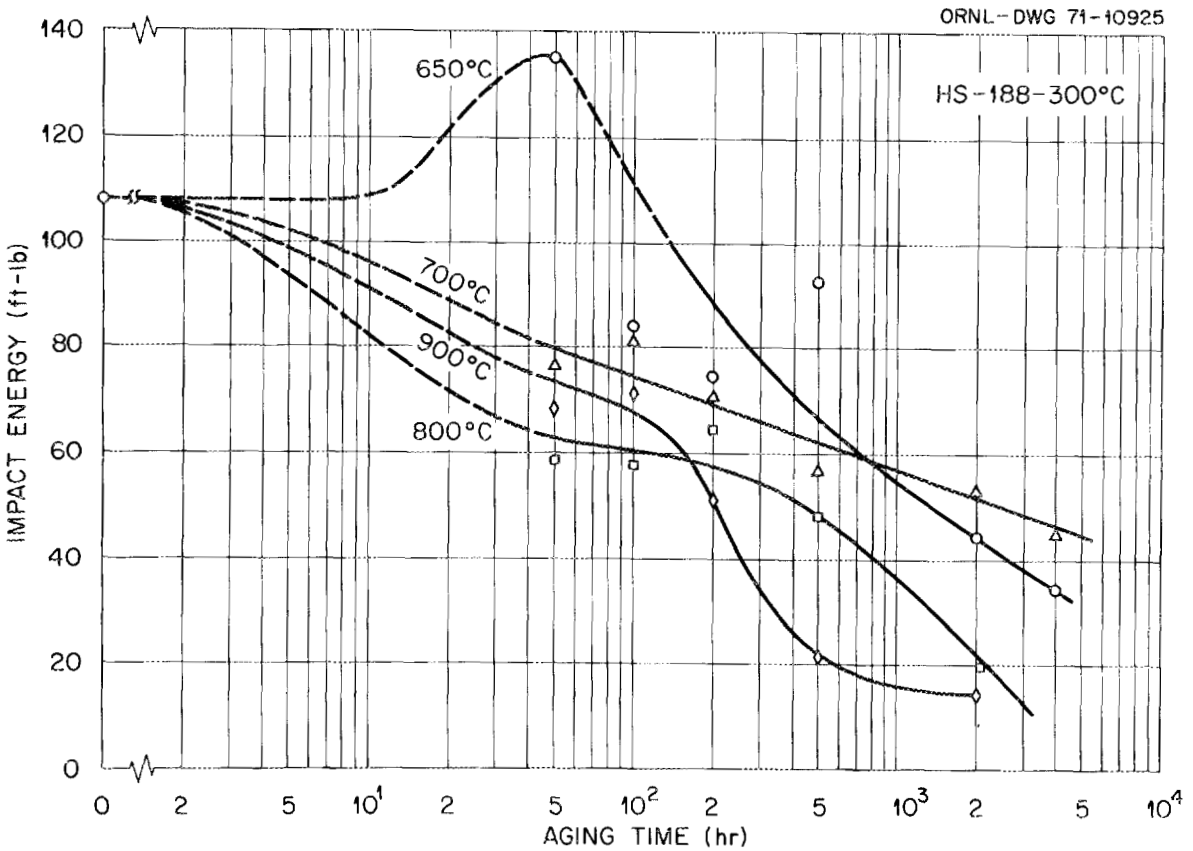

Fig. 8. Variation of Notch-Impact Energy at 300°C With Aging Time for Haynes Alloy No. 188. Samples annealed 1 hr at 1150°C before aging.

The fracture surfaces of the Haynes alloy No. 188 samples shown in Fig. 9 show the decrease in ductility with aging. The fracture appearance changed from fibrous to granular, and the reduction in width at the base of the notch decreased as the aging time increased.

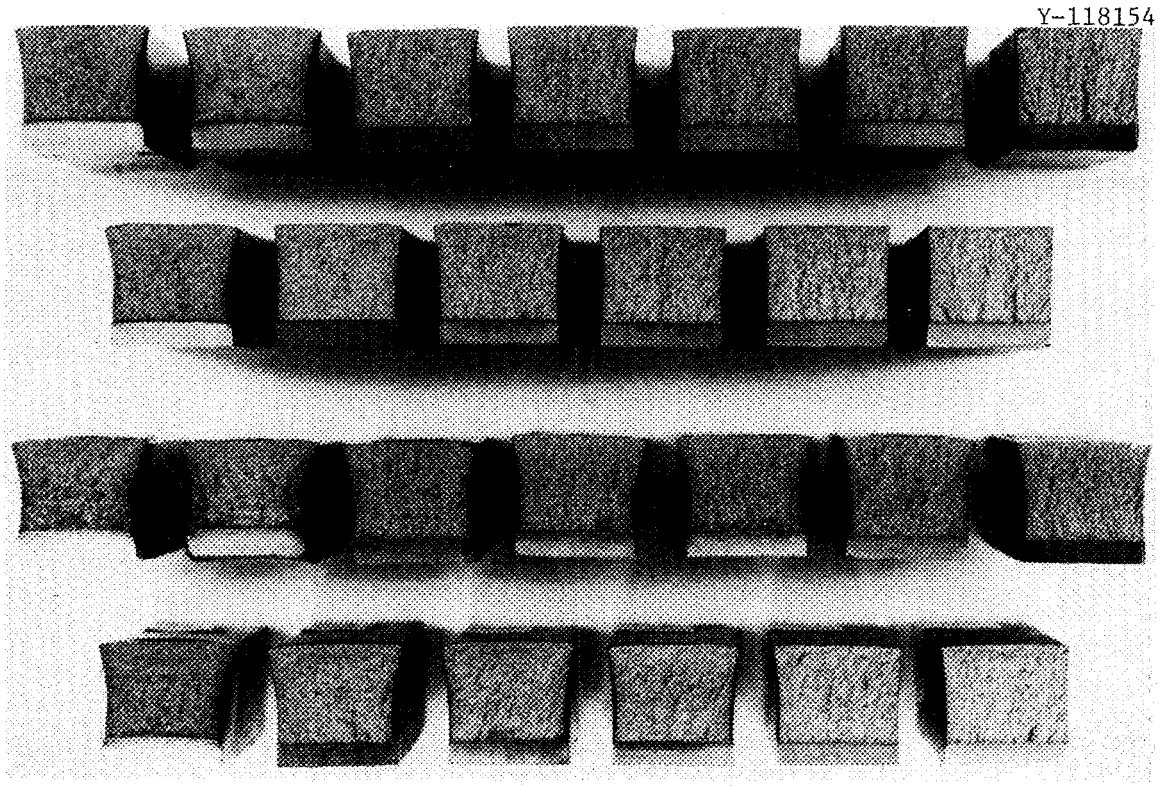

Fig. 9. Fracture Surfaces of Haynes Alloy No. 188 Impact Specimens. The aging time increases in each row from zero on the left to 4000 hr on the right. The samples in the top row were aged at 650°C and tested at 25°C, those in the second row were aged at 900°C and tested at 25°C, those in the third row were aged at 650°C and tested at 300°C, and those in the bottom row were aged at 900°C and tested at 300°C.

TENSILE PROPERTIES

Small tensile specimens having a gage section 1/2 in. long and 1/8 in. in diameter were machined from halves of several tested impact specimens. These specimens were tensile tested at 25°C at a strain rate of 0.1/min, and the results are summarized in Table 2. Although aging Hastelloy N at 900°C for 100 hr reduced the impact energy from 164 to 82 ft-lb (Fig. 1, p. 4) the uniaxial tensile properties changed very little (Table 2, specimens 11440 and 11441). Aging for 4000 hr at 900°C reduced the impact energy to 35 ft-lb, and the tensile properties indicate a general decrease in yield and tensile strength, very small changes in axial strain, and a sizeable decrease in the reduction in area (Table 2, specimens 11440 and 11448).

The tensile properties of Haynes alloy No. 25 were changed markedly as a result of aging. Aging for 50 hr at 850°C increased the yield stress

Table 2. Results of Tensile Tests at 25°C

Specimen	Aging[a]		Stress, psi			Strain, %		Reduction in Area, %
	(hr)	(°C)	Yield	Ultimate Tensile	Fracture	Uniform	Total	
				Hastelloy N				
11440	0		60,300	114,400	105,700	51.2	55.6	41.5
11441	100	900	59,000	118,100	112,300	50.5	54.4	41.5
11448	4000	900	55,500	106,800	100,200	41.5	56.4	27.7
				Haynes Alloy No. 25				
11446	0		71,700	138,400	137,500	43.2	43.6	27.9
11447	50	850	79,900	113,300	113,300	14.4	14.6	9.1
11445	4843	850	87,500	133,000	133,000	12.7	12.9	5.8
				Haynes Alloy No. 188				
11444	0		69,800	143,700	141,200	51.2	53.5	40.0
11443	100	900	69,200	139,300	138,500	37.0	37.9	27.3
11442	2000	900	71,100	137,300	137,300	21.1	21.6	7.7

[a]All specimens solution annealed 1 hr at 1150°C before aging.

and decreased all the ductility parameters (Table 2, specimens 11446 and 11447). These same aging conditions caused the impact energy to decrease from 70 to 6 ft-lb (Fig. 4, p. 5). Aging for 4843 hr at 850°C caused the yield stress to increase and the ductility parameters to decrease further. These same aging conditions caused the impact energy to decrease to about 3 ft-lb.

Aging at 900°C caused very little change in the strength parameters of Haynes alloy No. 188 (Table 2, specimens 11444, 11443, and 11442). However, the ductility parameters decreased with aging. The impact properties after 0, 100, and 2000 hr aging at 900°C were 58, 27, and 6 ft-lb, respectively (Fig. 7, p. 7).

METALLOGRAPHIC EXAMINATION

No phase identification work was done on these samples, so we will only indicate the phases that are likely present on the basis of other studies. Carbides of the M_2C and M_6C types are formed[1] in Hastelloy N, but the M_2C type should predominate in a heat such as 6960, which contained only 0.05% Si. The "M" in this carbide consists of about 80% Mo and 20% Cr. The microstructure of Hastelloy N after solution heat treatment is shown in Fig. 10. The grain boundaries were quite jagged and contained some fine carbide. Some coarser primary carbide was also present within the grains. Aging at 650°C caused a decrease in the impact energy for the first 500 hr and a slight increase with further aging (Fig. 1, p. 4). The microstructural change observed at 650°C was carbide precipitation along the grain boundaries, and no obvious characteristic of this precipitation could account for the slight minimum in the impact energy. Figure 11 shows the microstructure after 4000 hr aging at 650°C. Carbide has precipitated on and adjacent to the grain

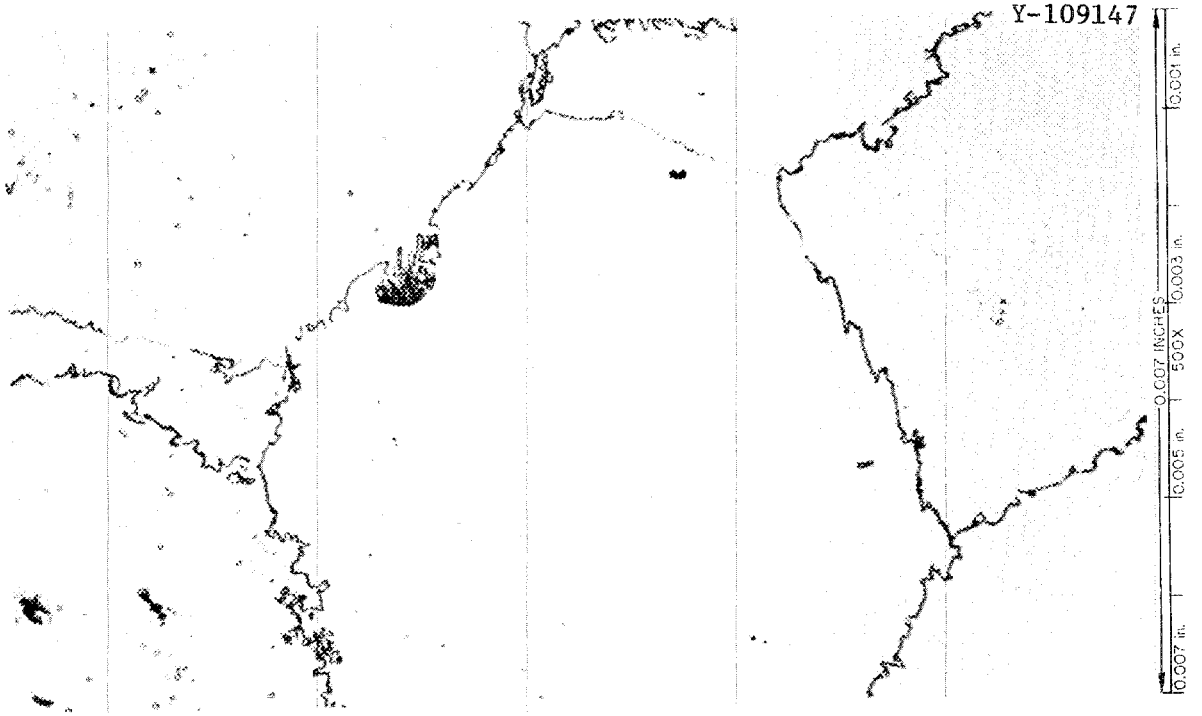

Fig. 10. Typical Photomicrograph of Hastelloy N Annealed 1 hr at 1150°C. Impact energy at 25°C was 164 ft-lb. Etchant: glyceria regia.

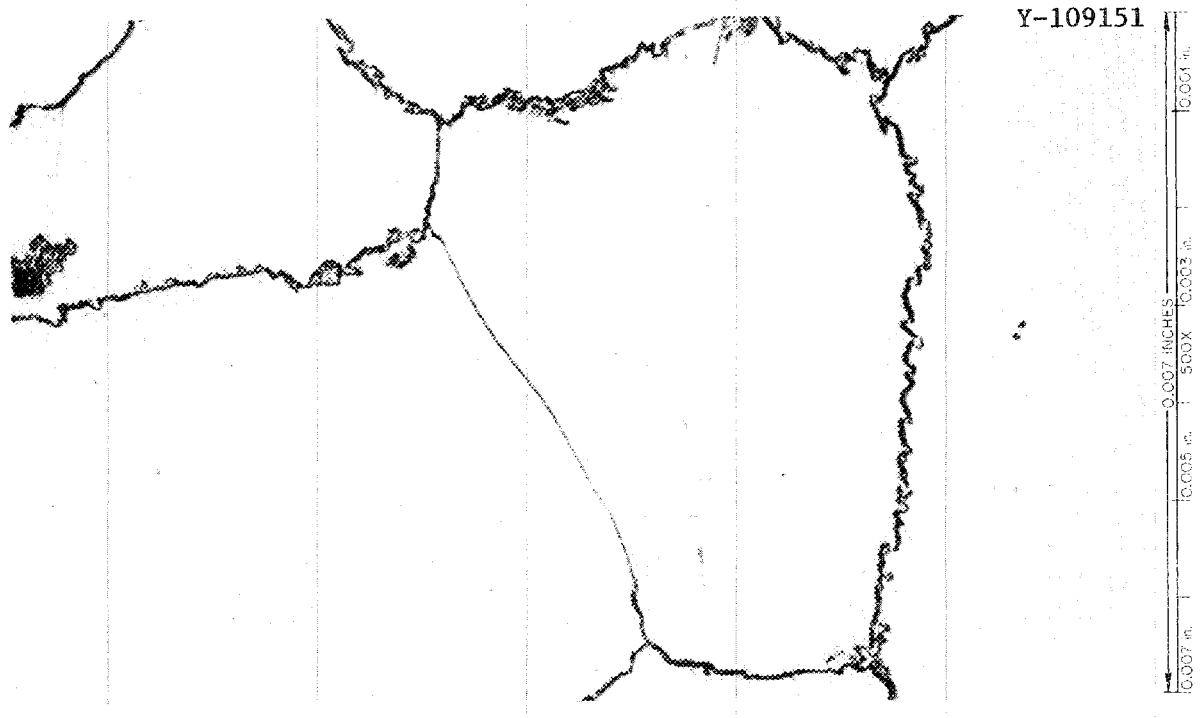

Fig. 11. Typical Photomicrograph of Hastelloy N Annealed 1 hr at 1150°C and Aged 4000 hr at 650°C. Impact energy at 25°C was 108 ft-lb. Etchant: glyceria regia.

boundaries. Aging at 700°C caused carbide precipitation similar to that noted at 650°C. Aging at 800°C initially caused grain boundary carbide precipitation and some general precipitation (Fig. 12). After prolonged aging at 800°C, the grain boundary carbide agglomerated, and the amount of precipitate within the grain increased (Fig. 13). However, the impact energy continued to decrease with further aging at 800°C (Fig. 1, p. 4) even though the grain boundary carbide appeared to become discontinuous. At 900°C the carbide formed preferentially along the grain boundaries (Fig. 14). It was initially quite fine and became coarser and agglomerated with further aging time. The impact energy decreased with increasing carbide formation and seemed to reach a plateau of about 30 ft-lb after the carbide became quite coarse (Fig. 1, p. 4).

Wlodek[3] has studied the embrittlement of Haynes alloy No. 25 and the phases that are formed. He found that the solution-annealed alloy contained M_6C and Zr(N,C). Aging over the range 650 to 1100°C formed $Cr_{23}C_6$ and a Laves phase, A_2B. After prolonged aging the major constituents were M_6C and the Laves phase. These various microconstituents assumed different morphologies at different aging temperatures, so it is not possible to identify microconstituents solely by optical metallography, and our phase identifications are largely conjecture.

The microstructure of solution-annealed Haynes alloy No. 25 is shown in Fig. 15; it contains a primary carbide, likely M_6C. Even though aging at 650°C caused a steady decrease in the impact energy from 60 to 2 ft-lb (Fig. 4, p. 5), the microstructure changed only slightly. After aging for 4843 hr at 650°C (Fig. 16) the grain boundaries etched very quickly (likely because of the presence of carbide or Laves precipitate), and some precipitate was visible in the grains. Aging at 700°C produced a steady decrease in the impact energy (Fig. 4, p. 5), and large amounts of precipitate (likely Laves phase) were visible in the microstructure (Fig. 17). Aging at 800°C resulted in coarser precipitate than noted at 700°C, and the grain boundaries etched very readily (Fig. 18). Aging at 850°C for 50 hr caused the impact energy to decrease from 50 to 6 ft-lb (Fig. 4, p. 5), but the microstructure showed little change from the solution-annealed condition (compare Figs. 15 and 19). The main difference is the more rapid etching characteristics of the grain boundaries after aging. Aging 4843 hr at 850°C caused the impact energy to decrease only slightly from that noted after aging 50 hr; however, the amount of precipitate increased dramatically (Fig. 20). These observations lead to the speculation that the impact property changes in Haynes alloy No. 25 result primarily from the grain boundary precipitate structure and to a lesser extent on the precipitate within the grains.

Herchenroeder[4] studied the aging characteristics of four heats of Haynes alloy No. 188. He found that the solution-annealed alloy contained primary M_6C and that aging formed secondary M_6C, $M_{23}C_6$, and a Laves phase of the A_2B type. Over the range 700 to 900°C the M_6C tended strongly to transform to $M_{23}C_6$ on aging. The carbide transformation would make more of the group VIB materials available to form the A_2B phase.

Aging at 650°C caused the impact energy of Haynes alloy No. 188 to decrease (Fig. 7, p. 7). The microstructure changed very little during the 2000 hr aging (Fig. 21). The primary change was the formation of precipitates along the grain boundaries so that these regions etched

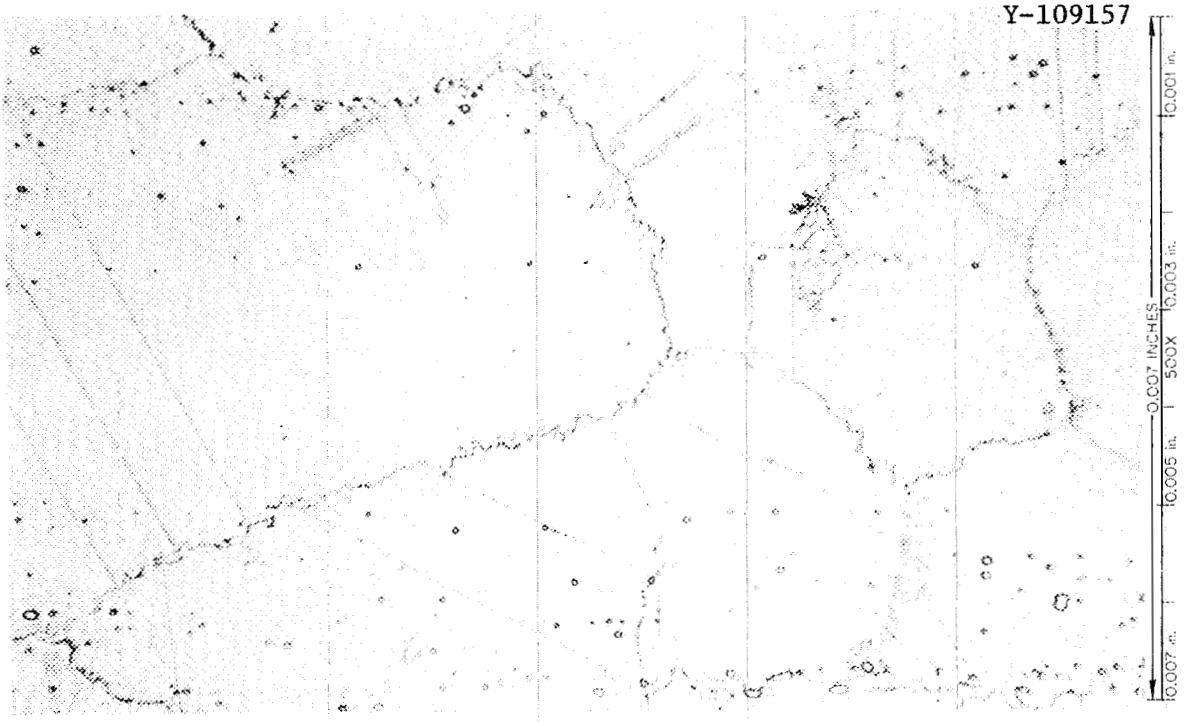

Fig. 12. Typical Photomicrograph of Hastelloy N Annealed 1 hr at 1150°C and Aged 100 hr at 800°C. Impact energy was 165 ft-lb. Etchant: glyceria regia.

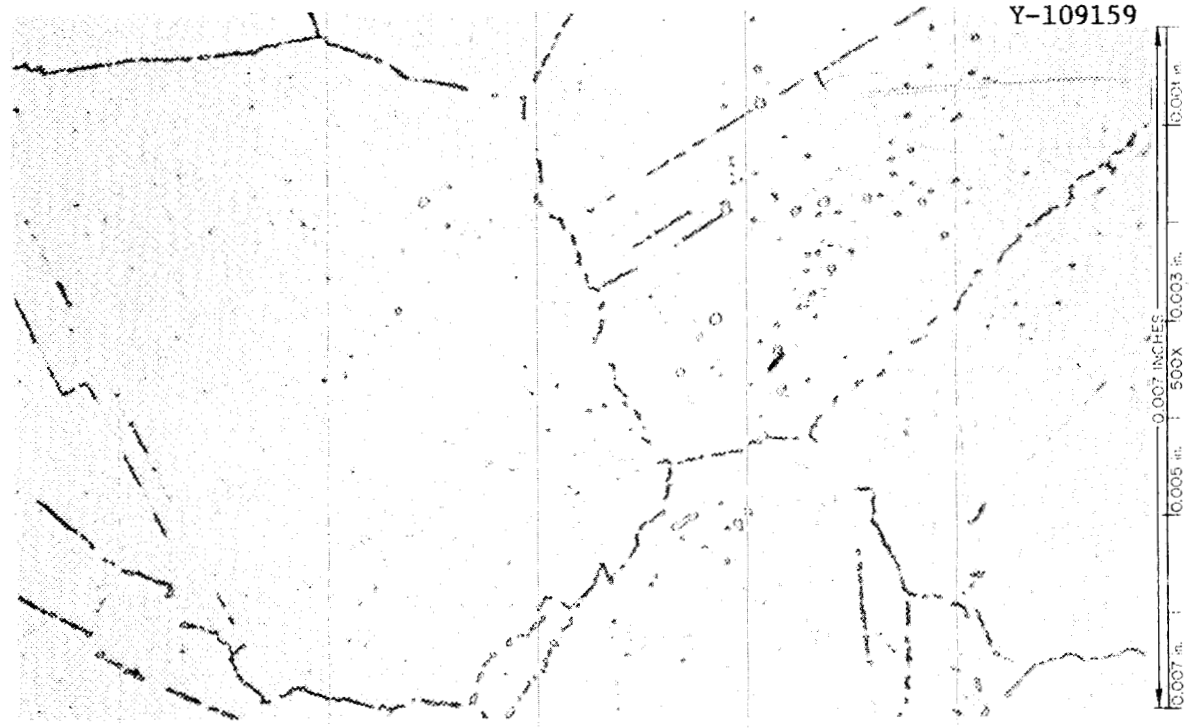

Fig. 13. Typical Photomicrograph of Hastelloy N Annealed 1 hr at 1150°C and Aged 4000 hr at 800°C. Impact energy was 40 ft-lb. Etchant: glyceria regia.

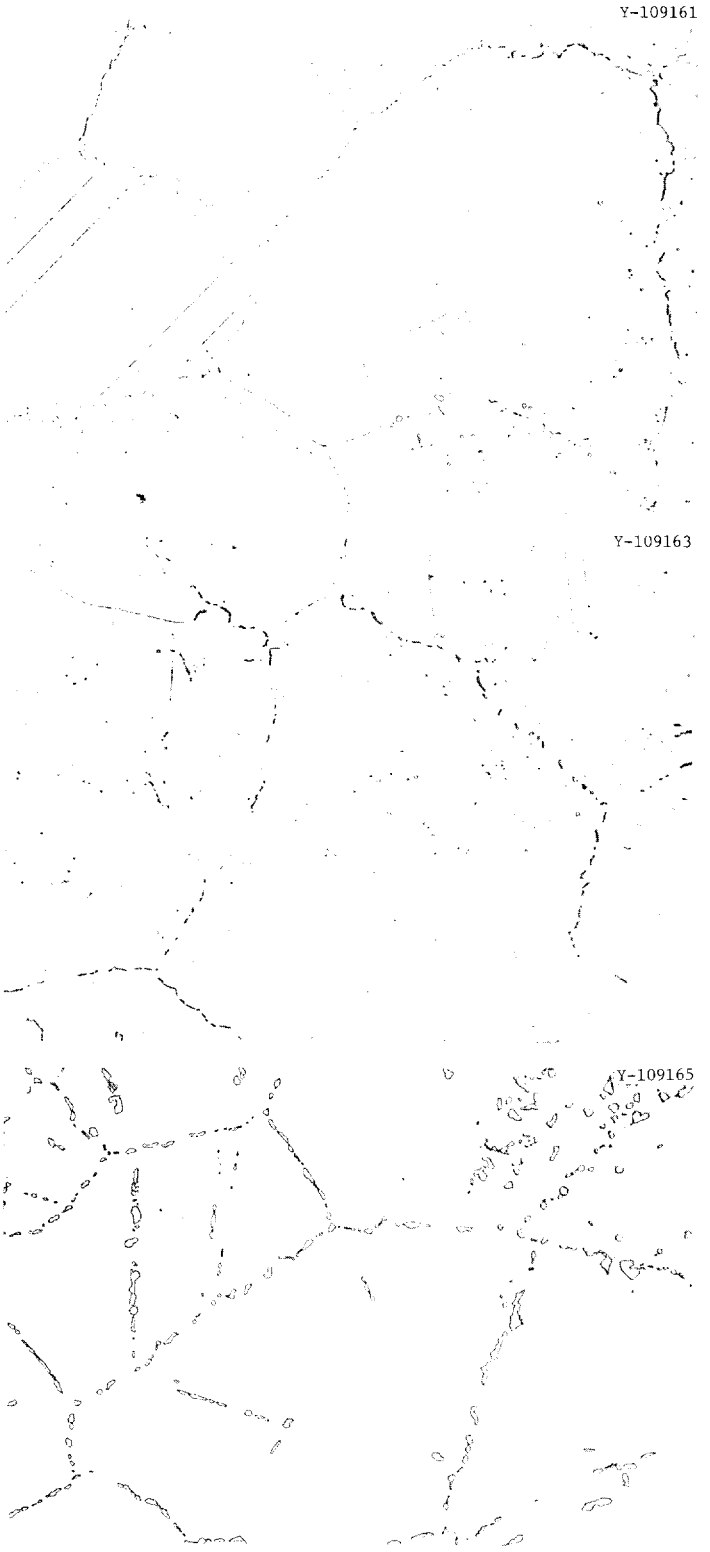

Fig. 14. Photomicrographs of Hastelloy N Annealed 1 hr at 1150°C and Aged at 900°C. 500×. (Reduced 39.5%). (a) 50 hr, (b) 100 hr, and (c) 4000 hr. Impact energies at 25°C were 114, 83, and 36 ft-lb, respectively. Etchant: glyceria regia.

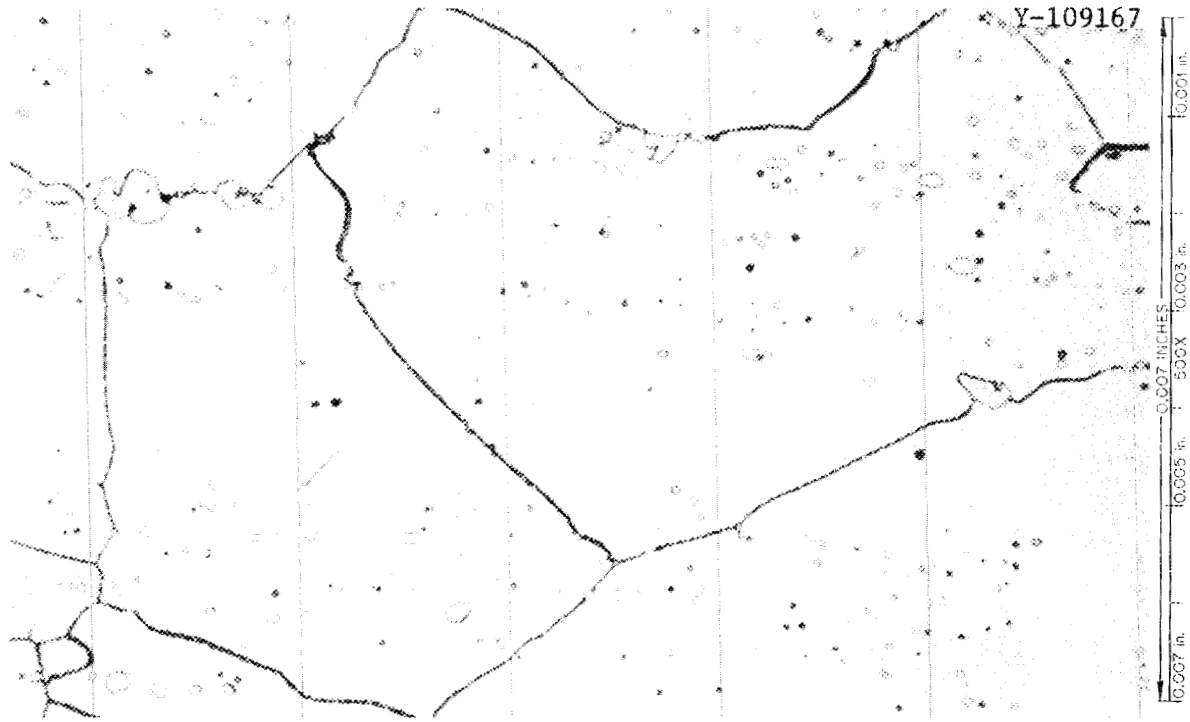

Fig. 15. Typical Photomicrograph of Haynes Alloy No. 25 Annealed 1 hr at 1150°C. Impact energy at 25°C was 70 ft-lb. Etchant: glyceria regia.

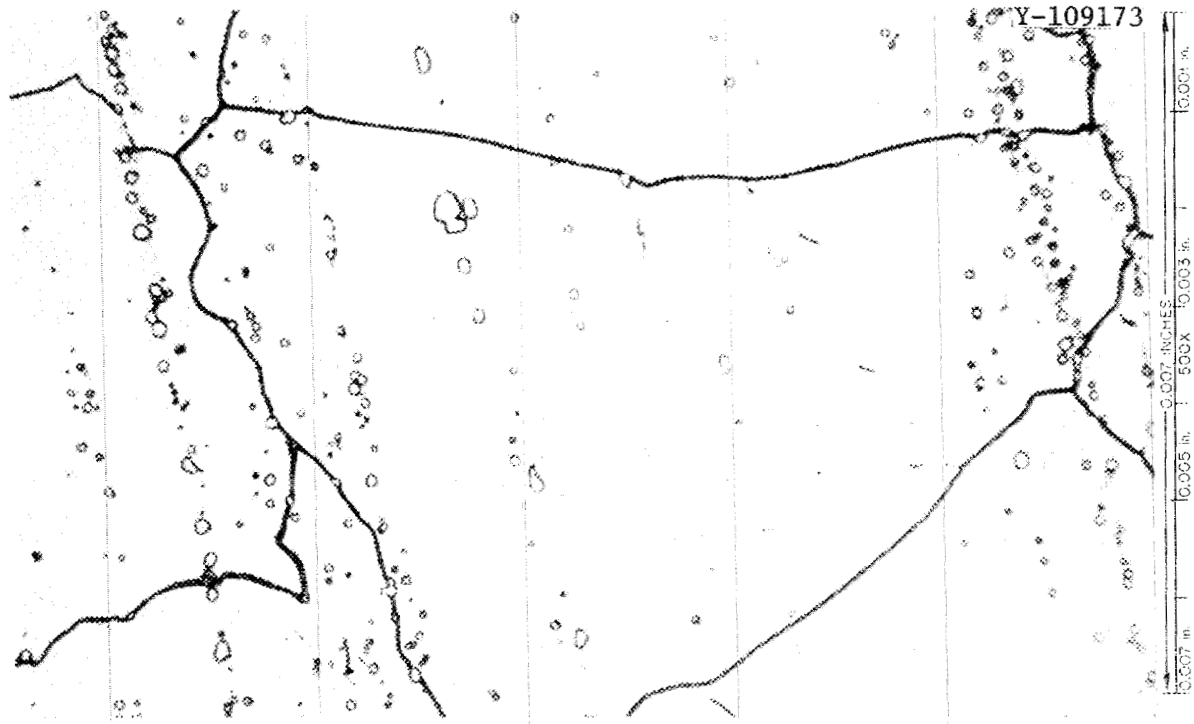

Fig. 16. Typical Photomicrograph of Haynes Alloy No. 25 Annealed 1 hr at 1150°C and Aged 4843 hr at 650°C. Impact energy at 25°C was 2 ft-lb. Etchant: glyceria regia.

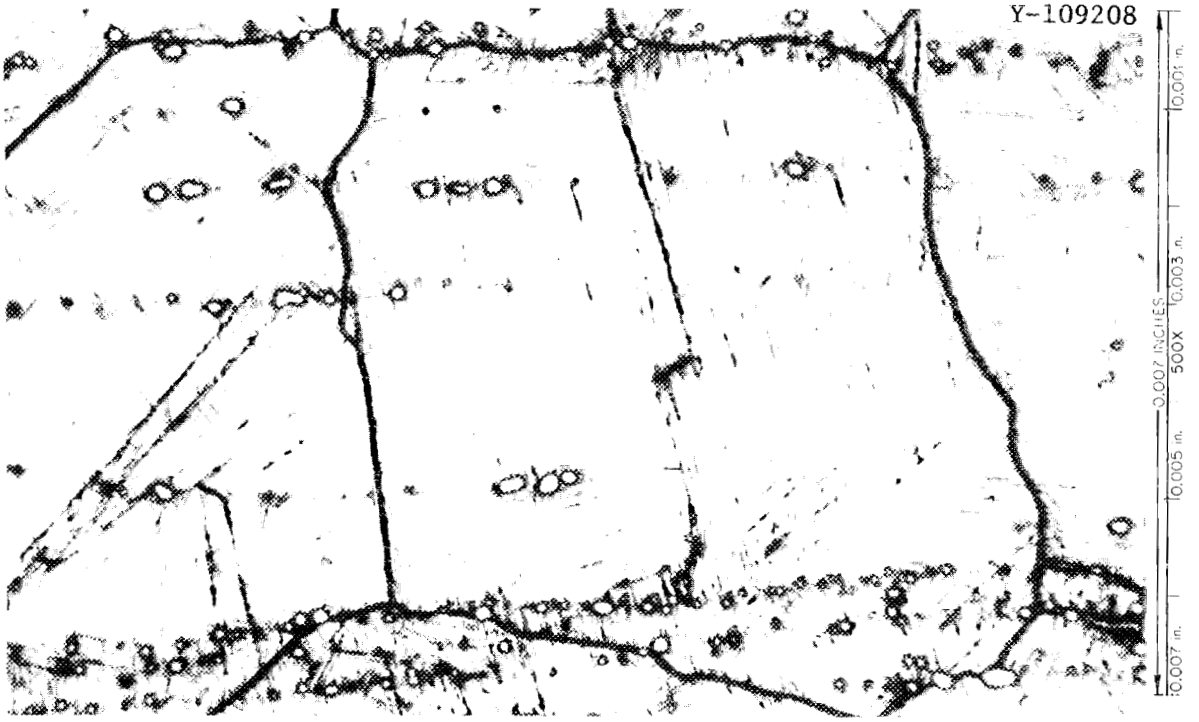

Fig. 17. Typical Photomicrograph of Haynes Alloy No. 25 Annealed 1 hr at 1150°C and Aged 4843 hr at 700°C. Impact energy at 25°C was 5 ft-lb. Etchant: glyceria regia.

Fig. 18. Typical Photomicrograph of Haynes Alloy No. 25 Annealed 1 hr at 1150°C and Aged 4843 hr at 800°C. Impact energy at 25°C was 7 ft-lb. Etchant: glyceria regia.

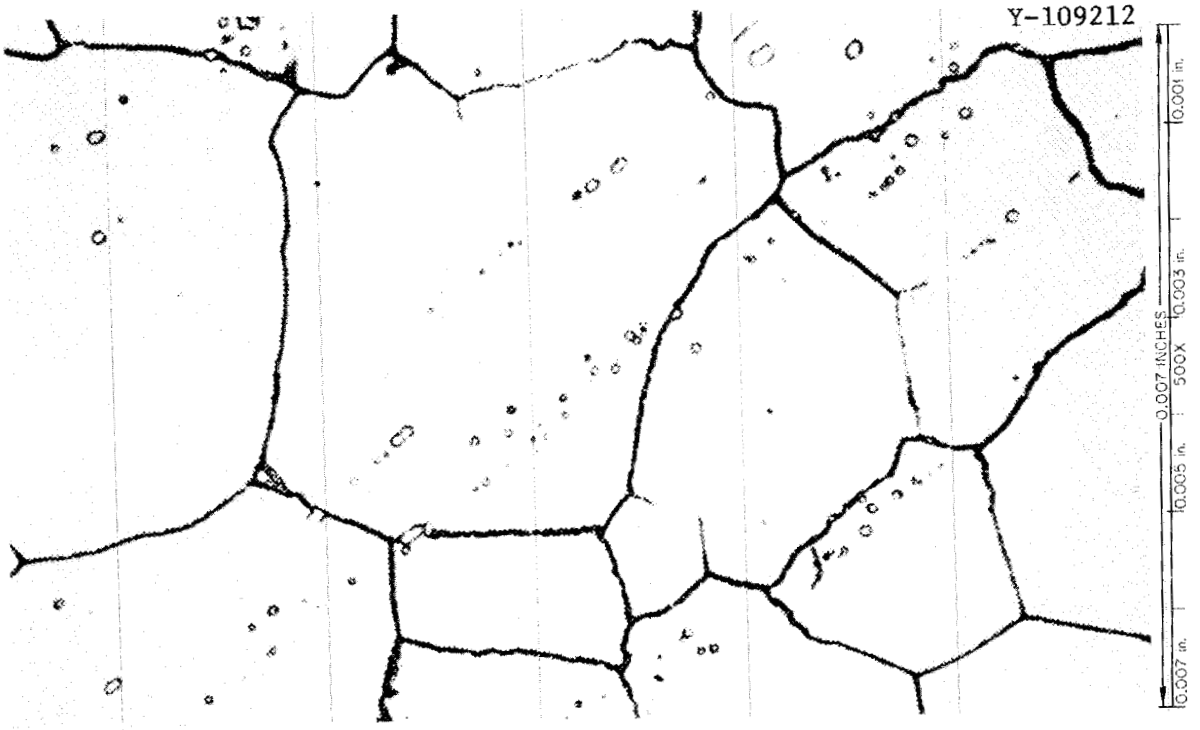

Fig. 19. Typical Photomicrograph of Haynes Alloy No. 25 Annealed 1 hr at 1150°C and Aged 50 hr at 850°C. Impact energy at 25°C was 6 ft-lb. Etchant: glyceria regia.

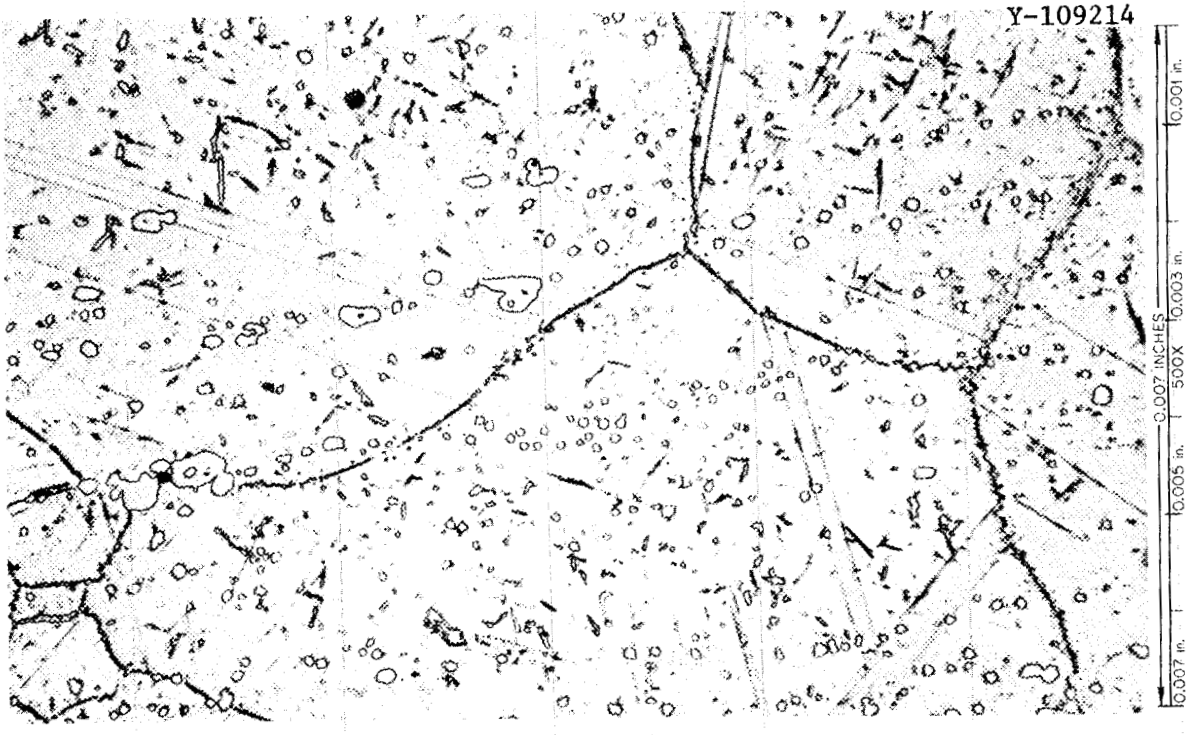

Fig. 20. Typical Photomicrograph of Haynes Alloy No. 25 Annealed 1 hr at 1150°C and Aged 4843 hr at 850°C. Impact energy at 25°C was 3 ft-lb. Etchant: glyceria regia.

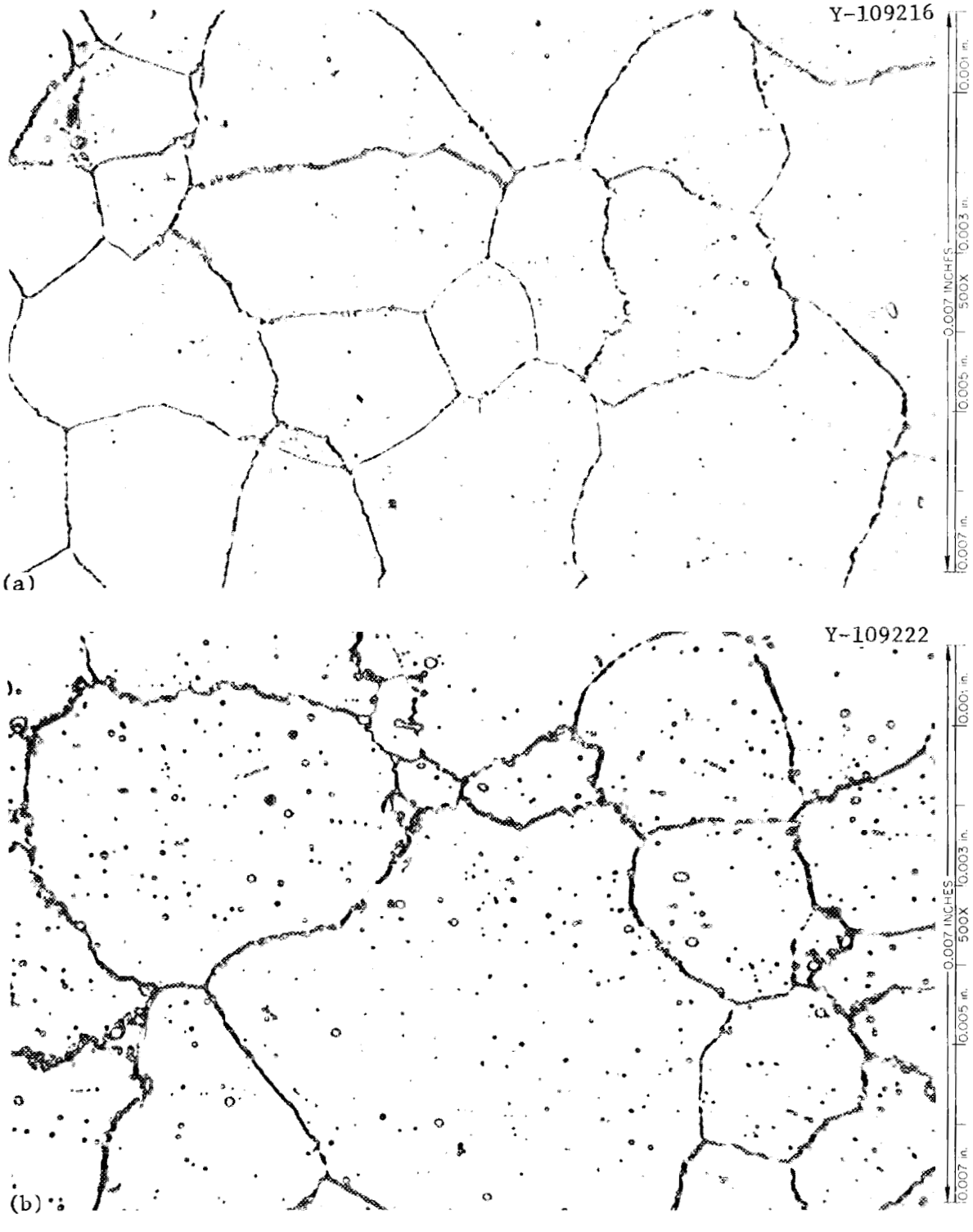

Fig. 21. Typical Photomicrographs of Haynes Alloy No. 188.
(a) Annealed 1 hr at 1150°C. Impact energy at 25°C was 59 ft-lb.
(b) Annealed 1 hr at 1150°C and aged 2000 hr at 650°C. Impact energy at 25°C was 22 ft-lb. Etchant: glyceria regia.

more readily. The results of Herchenroeder[4] indicate that a sample aged at 650°C would contain $M_{23}C_6$ and M_6C, but likely not Laves phase. The microstructure resulting from 2000 hr aging at 700°C contained copious grain boundary precipitate, likely carbides (Fig. 22). Aging at 800°C for 2000 hr resulted in the formation of more precipitates, primarily grain boundary (Fig. 23). Herchenroeder's work would indicate that this sample contained $M_{23}C_6$ and Laves phase. Aging at 900°C caused the grain boundary precipitate to agglomerate and a large amount of precipitate to form within the grains (Fig. 24). The samples in Fig. 24 likely contain $M_{23}C_6$, M_6C, and Laves phase.

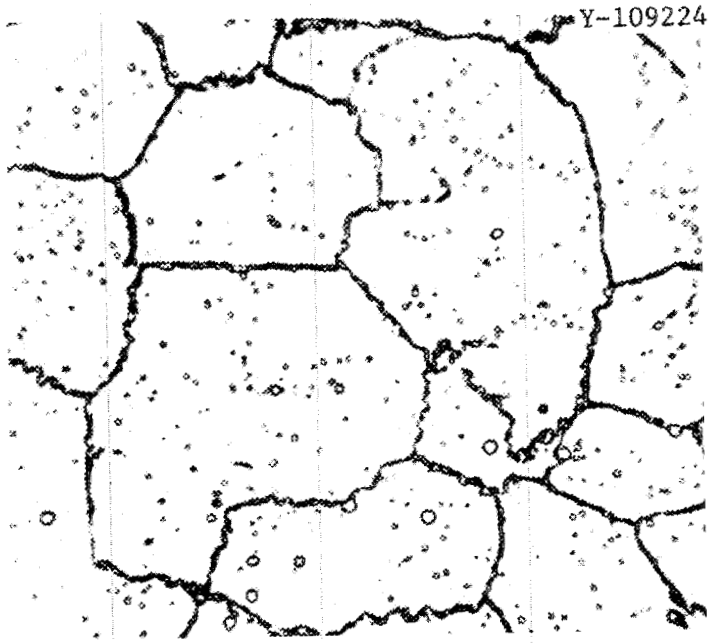

Fig. 22. Typical Photomicrograph of Haynes Alloy No. 188 Annealed 1 hr at 1150°C and Aged 2000 hr at 700°C. Impact energy at 700°C was 24 ft-lb. Etchant: glyceria regia. 500×.

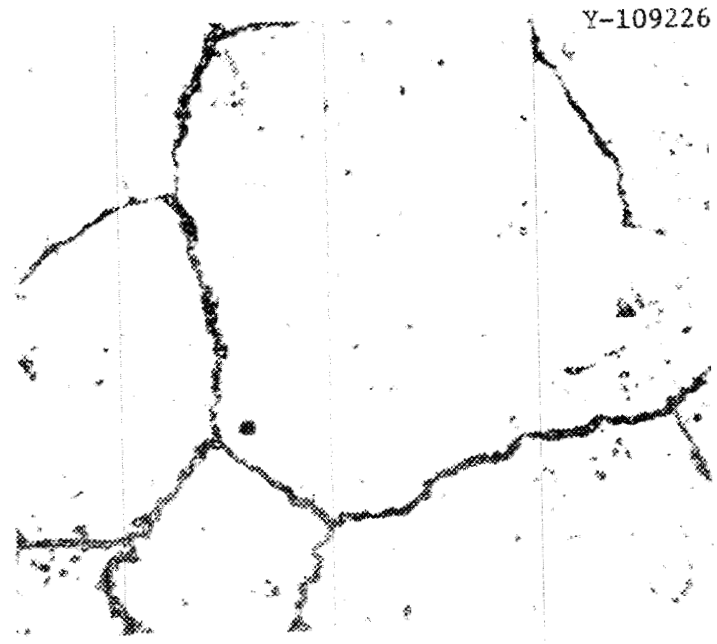

Fig. 23. Typical Photomicrograph of Haynes Alloy No. 188 Annealed 1 hr at 1150°C and Aged 2100 hr at 800°C. Impact energy at 25°C was 9 ft-lb. Etchant: glyceria regia. 500×.

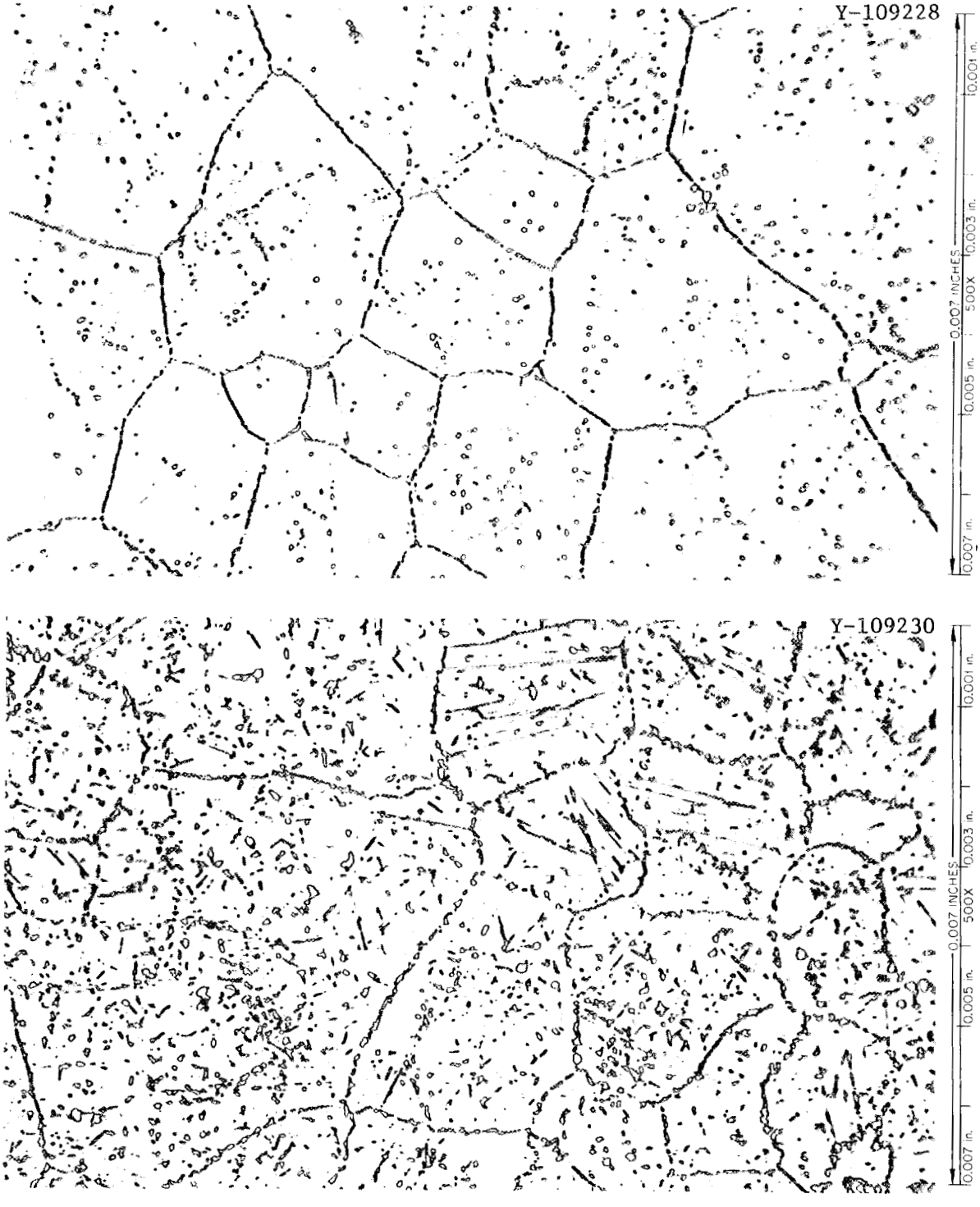

Fig. 24. Typical Photomicrographs of Haynes Alloy No. 188 Annealed 1 hr at 1150°C and Aged at 900°C. (a) Aged 100 hr, impact energy at 25°C was 28 ft-lb. (b) Aged 2000 hr, impact energy at 25°C was 6 ft-lb. Etchant: glyceria regia.

SCANNING ELECTRON MICROSCOPE OBSERVATIONS

The fractures of the nine tensile samples described in Table 2 (p. 10) were examined in the scanning electron microscope. Typical views of the Hastelloy N fractures are shown in Fig. 25. Some portions of the fracture were intergranular, but the entire surface shows deformation markings characteristic of ductile fracture. The intergranular cracks perpendicular to the plane of view would be expected because of the complex stress state that developed before fracture. As the specimen necked, three-dimensional stresses developed that would tend to open cracks perpendicular to the applied stress. The features of the fracture surface changed very little as a result of aging.

The photomicrographs shown in Fig. 26 of the Haynes alloy No. 25 tensile specimens show that the fractures are primarily intergranular. The main change that occurred with aging was a reduction in the amount of deformation (evidenced by dimpling) that occurred before fracture.

The fracture surfaces of the Haynes alloy No. 188 tensile specimens shown in Fig. 27 are quite similar to those of Haynes alloy No. 25. The predominant difference is the more ductile appearance of the Haynes alloy No. 188. Although the fractures were almost entirely intergranular, the fracture surfaces are dimpled from plastic deformation. We saw no features in Fig. 27 that obviously changed with aging, although the reduction in area changed from 40.0 to 7.7%.

DISCUSSION OF RESULTS

All three alloys underwent substantial losses in toughness as a result of aging over the temperature range 650 to 900°C. Hastelloy N forms only carbides during aging, but the alloy lost about 80% of its toughness during aging at 800 and 900°C (Fig. 1, p. 4). Aging at 650 and 700°C caused losses of about 50%. These losses in toughness seem to correlate with the amount of grain boundary precipitate.

Haynes alloys Nos. 25 and 188 are more complex than Hastelloy N in that they form Laves phases. The aging characteristics of these two alloys are compared in Fig. 28 in terms of the reduction in the impact energy. One of the objectives in the development of alloy No. 188 was to reduce the embrittlement due to Laves phase that occurred in Haynes alloy No. 25. The comparison in Fig. 28 shows that this was partially successful, since the time required to cause a certain loss in impact energy was much greater for alloy No. 188. This is particularly true for the larger losses in impact energy. For example, at 800°C alloy No. 25 lost 75% of its impact energy in 30 hr, but alloy No. 188 required 600 hr.

Haynes alloys Nos. 25 and 188 both formed Laves phase, but alloy No. 188 formed less. Both alloys formed carbides. The toughness of a material can be reduced by the matrix or the grain boundaries becoming brittle so that a low-energy fracture path is defined. The carbide and Laves phases could produce either of these effects. It is quite likely, although not necessarily the case, that the formation of either phase in quantities sufficient to embrittle the matrix would harden it also. It is also possible for the matrix to be strengthened sufficiently to cause the grain boundaries and adjacent regions to deform preferentially to the

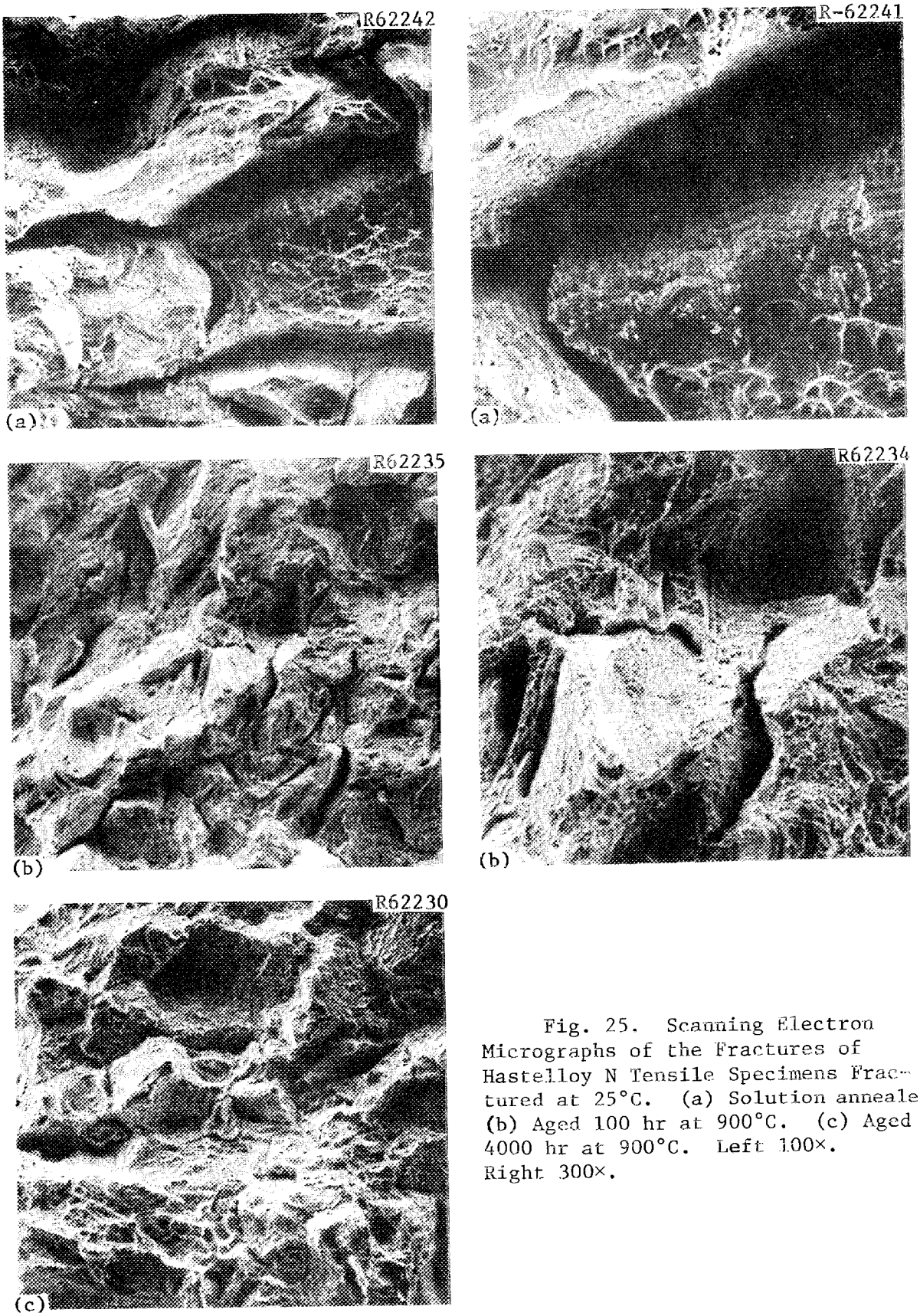

Fig. 25. Scanning Electron Micrographs of the Fractures of Hastelloy N Tensile Specimens Fractured at 25°C. (a) Solution annealed. (b) Aged 100 hr at 900°C. (c) Aged 4000 hr at 900°C. Left 100×. Right 300×.

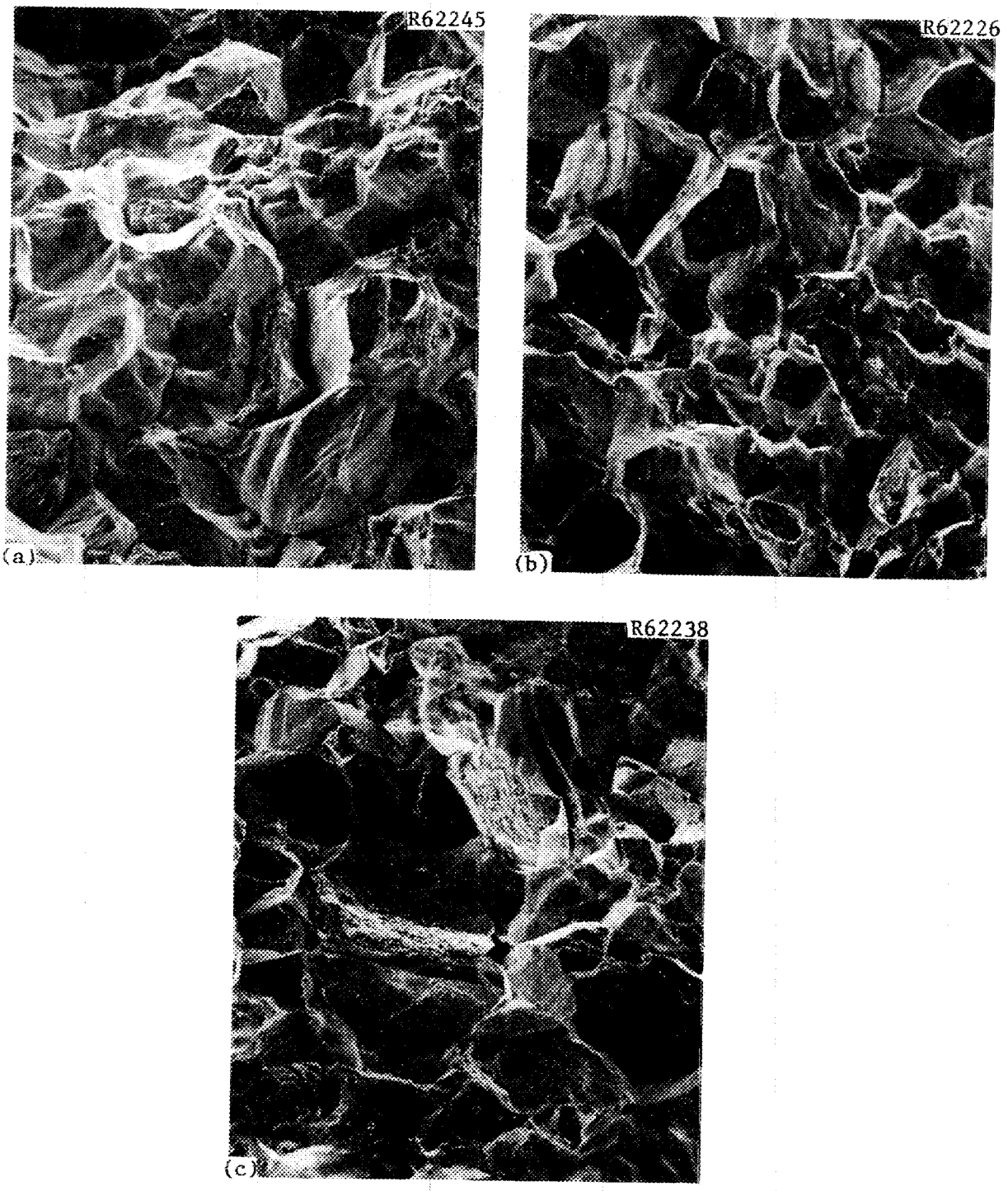

Fig. 26. Scanning Electron Micrographs of the Fractures of Haynes Alloy No. 25 Tensile Specimens Fractured at 25°C. 100×. (a) Solution annealed. (b) Aged 50 hr at 850°C. (c) Aged 4843 hr at 850°C.

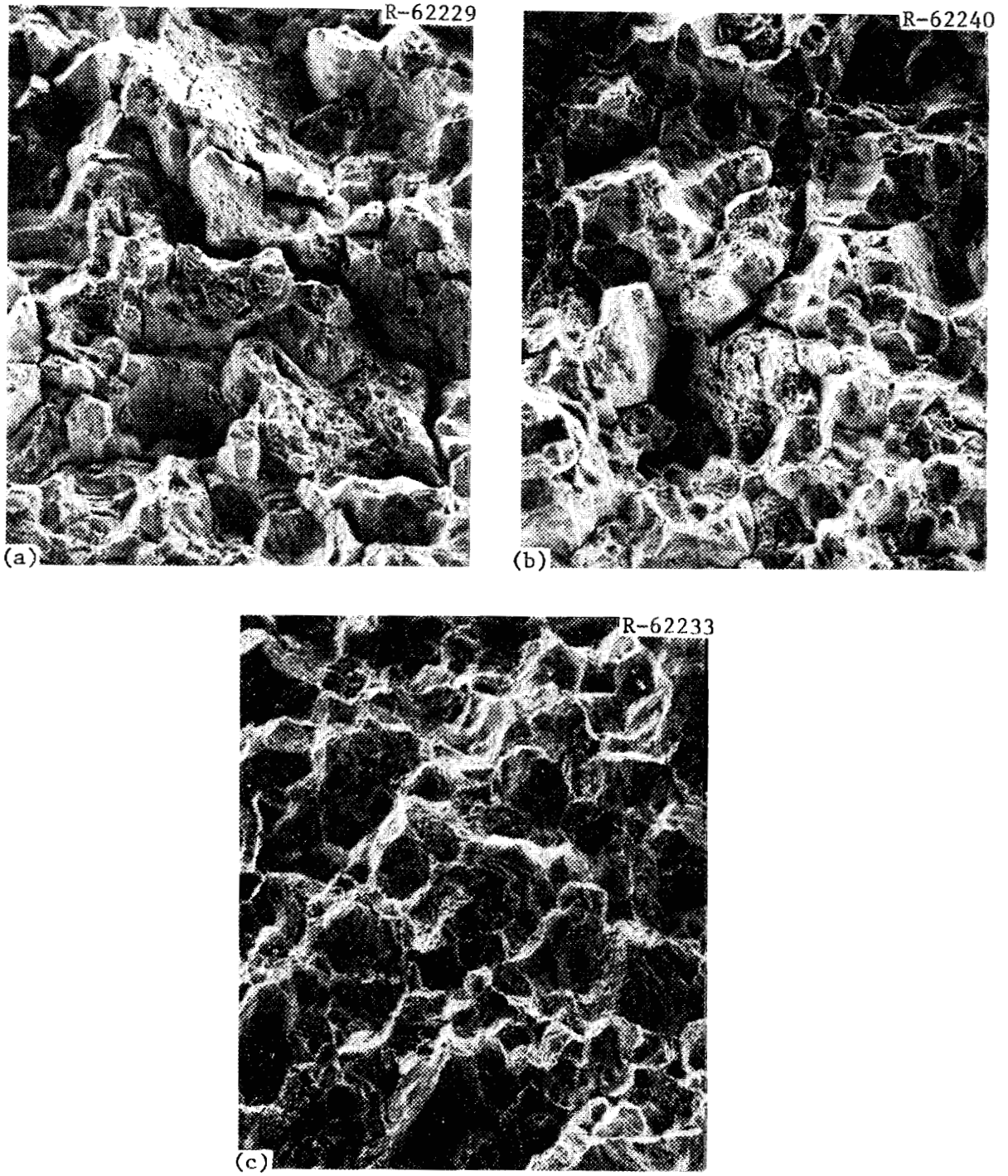

Fig. 27. Scanning Electron Micrographs of the Fractures of Haynes Alloy No. 188 Tensile Specimens Tested at 25°C. 100×. (a) Solution annealed. (b) Aged 100 hr at 900°C. (c) Aged 2000 hr at 900°C.

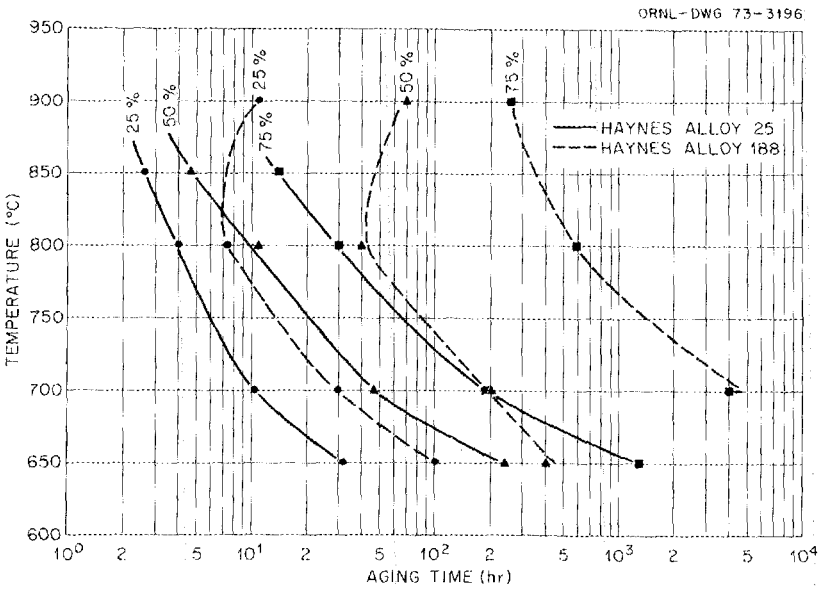

Fig. 28. Reduction in Impact Energy at 25°C Due to Aging for Haynes Alloys Nos. 25 and 188. All samples annealed 1 hr at 1150°C before aging.

matrix. The yield stress of Haynes alloy No. 25 (Table 1, p. 3) increased about 20% with aging, and the ductility parameters decreased. This alloy showed a strong tendency to fail intergranularly in the solution-annealed condition, and the tendency toward intergranular fracture increased. There was less evidence of grain boundary plasticity with aging, indicating that the grain boundaries themselves became less ductile with aging. The stronger matrix may have contributed to the embrittlement, but the grain boundary embrittlement seemed to be the dominant factor.

The data for Haynes alloy No. 188 are even less definitive of an embrittlement mechanism. The solution-annealed material fractured predominantly intergranularly. The yield and tensile stresses changed very little during aging, but the ductility decreased (Table 2, p. 10). Although the fracture was intergranular, considerable deformation occurred before the fracture (Fig. 27), and this did not change appreciably with aging. Thus, there is no evidence to support the premises that the matrix was strengthened or that the grain boundaries were embrittled by aging.

SUMMARY

Impact samples of Hastelloy N, Haynes alloy No. 25, and Haynes alloy No. 188 were solution annealed and aged up to 4000 hr at temperatures over the range 650 to 900°C. Impact tests were run at 25 and 300°C, and all alloys underwent reduction in toughness due to aging. The reduction in toughness was least for Hastelloy N, intermediate for alloy No. 188, and greatest for alloy No. 25. The changes in Hastelloy N were due to carbide precipitation, and those in Haynes alloys Nos. 25 and 188

were likely due to the combined effects of carbide and Laves phase precipitation.

ACKNOWLEDGMENTS

The authors gratefully acknowledge the contributions of J. M. Newsome, T. N. Jones, and W. J. Stelzman for the aging and impact testing; H. R. Tinch for the metallography; R. G. Berggren, R. G. Donnelly, and W. R. Martin for review of the manuscript; the ORNL Graphic Arts Department for preparation of the drawings, and the Metals and Ceramics Division Reports Office for preparation of the manuscript.

REFERENCES

1. H. E. McCoy and R. E. Gehlbach, "Influence of Irradiation Temperature on the Creep-Rupture Properties of Hastelloy N," *Nucl. Technol.* 11(1): 45–60 (1971).

2. H. E. McCoy, Jr., *An Evaluation of the Molten-Salt Reactor Experiment Hastelloy N Surveillance Specimens — Fourth Group*, ORNL-TM-3063 (March 1971).

3. S. T. Wlodek, *Embrittlement of a Co-Cr-W (L-605) Alloy*, R-61-FPD-538 (December 1961).

4. R. B. Herchenroeder, *Aging Characteristics "Haynes" Developmental Alloy No. 188*, Report No. 7513, Technology Department, Stellite Division, Union Carbide, Kokomo, Indiana (August 1, 1968).

5. D. T. Bourgette, *Effect of Aging Time and Temperature on the Impact and Tensile Behavior of L-605 — A Cobalt-Base Alloy*, ORNL-TM-3734 (April 1973).

INTERNAL DISTRIBUTION
(73 copies)

(3) Central Research Library
ORNL — Y-12 Technical Library
Document Reference Section
(20) Laboratory Records Department
Laboratory Records, ORNL RC
ORNL Patent Office
G. M. Adamson, Jr.
R. G. Berggren
E. E. Bloom
C. R. Brinkman
D. A. Canonico
R. W. Carpenter
F. L. Culler
J. E. Cunningham
J. H. DeVan
J. R. DiStefano
(3) R. G. Donnelly
R. J. Gray
K. W. Haff
(3) M. R. Hill
D. O. Hobson
H. Inouye
R. T. King
C. C. Koch
E. Lamb
C. T. Liu
W. R. Martin
(5) H. E. McCoy
H. C. McCurdy
R. E. McDonald
C. J. McHargue
P. Patriarca
P. L. Rittenhouse
(3) R. A. Robinson
M. W. Rosenthal
A. C. Schaffhauser
J. L. Scott
G. M. Slaughter
W. J. Stelzman
J. O. Stiegler
R. W. Swindeman
D. B. Trauger
J. R. Weir, Jr.

EXTERNAL DISTRIBUTION
(79 copies)

AEC ALBUQUERQUE OPERATIONS OFFICE, P.O. Box 5400, Albuquerque, NM 87115

D. Ofte

AEC DAYTON AREA OFFICE, P.O. Box 66, Miamisburg, OH 45342

D. D. Davis

AEC DIVISION OF APPLIED TECHNOLOGY, Washington, DC 20545

W. S. Hollman
J. N. Maddox
R. W. Shivers

AEC DIVISION OF REACTOR RESEARCH AND DEVELOPMENT, Washington, DC 20545

T. A. Nemzek
T. C. Reuther
J. M. Simmons
E. E. Sinclair
A. Van Echo
C. E. Weber

AEC DIVISION OF SPACE NUCLEAR SYSTEMS, Washington, DC 20545

R. T. Carpenter
G. P. Dix
D. S. Gabriel
N. Goldenberg
H. Jaffe
W. K. Kern
A. P. Litman
G. A. Newby
F. Schulman
F. C. Schwenk
C. O. Tarr

AEC-RRD SITE REPRESENTATIVES, Oak Ridge National Laboratory, P.O. Box X, Oak Ridge, TN 37830

D. F. Cope
D. C. Davis, Jr.
C. L. Matthews

AIR FORCE MATERIALS LABORATORY, Wright-Patterson Air Force Base, OH 45433

L. N. Hjelm
I. Perlmutter

AIR FORCE SYSTEMS COMMAND (SCIZM), Andrews Air Force Base, MD 29331

G. R. Crane

AIR FORCE WEAPONS LABORATORY, Kirtland Air Force Base, Albuquerque, NM 87117

A. Noonan
M. MacWilliams

ALVAC METALS COMPANY, P.O. Box 759, Monroe, NC 28110

W. M. Thomas

ARGONNE NATIONAL LABORATORY, 9700 S. Cass Avenue, Argonne, IL 60439

R. W. Weeks

BATELLE MEMORIAL INSTITUTE, 505 King Avenue, Columbus, OH 43201

Defense Materials Information Center
W. Pardue

BUREAU OF MINES, ALBANY METALLURGY RESEARCH CENTER, P.O. Box 70, Albany, OR 97321

Haruo Kato

CABOT CORPORATION, STELLITE DIVISION, Kokomo, IN 46901

T. K. Roche
S. T. Wlodek

DONALD W. DOUGLAS LABORATORIES, 2955 George Washington Way, Richland WA 99352

D. Watrous

DUPONT COMPANY, Savannah River Laboratory, Aiken, SC 29801

D. R. Turno

GENERAL ELECTRIC COMPANY, SPACE DIVISION, ISOTOPE POWER SYSTEMS OPERATIONS, P.O. Box 8661, Philadelphia, PA 19101

Paul Brown
H. Sayell
R. E. Schafer

GULF GENERAL ATOMIC, P.O. Box 608, San Diego, CA 92112

N. B. Elsner
L. Yang

HUNTINGTON ALLOYS, Huntington, WV 25720

J. M. Martin

ISOTOPES, INC., NUCLEAR SYSTEMS DIVISION, 110 W. Timonium Road, Timonium, MD 21093

G. Linkous

JET PROPULSION LABORATORY, 4800 Oak Grove Drive, Pasadena, CA 91103

R. G. Ivanoff
V. Truscello

JOHNS HOPKINS UNIVERSITY, Department of Mechanics, Baltimore, MD 21218

R. Fischell

LOS ALAMOS SCIENTIFIC LABORATORY, P.O. Box 1663, Los Alamos, NM 87544

R. D. Baker
K. Cooper
R. Mulford

MONSANTO RESEARCH CORPORATION, MOUND LABORATORY, P.O. Box 32, Miamisburg, OH 45342

V. L. Avona
W. T. Cave
E. W. Johnson
P. Tucker

NASA, AMES RESEARCH CENTER, Moffett Field, CA 94035

H. Nelson
A. Wilbur

NASA, GODDARD SPACE FLIGHT CENTER, Greenbelt, MD 20770

J. Epstein

NASA HEADQUARDERS, CODE RN, 600 Independence Avenue, Washington, DC 20545

G. Deutsch
T. B. Kerr

NASA, LANGLEY RESEARCH CENTER, Langley Station, Hampton, VA 23365

R. Brouns

NASA, LEWIS RESEARCH CENTER, 21000 Brookpart Road, Cleveland, OH 44135

G. M. Ault
H. C. Slone

NASA, MANNED SPACECRAFT CENTER, Mail Code E-P5, Houston, TX 77058

T. W. Redding

NAVAL AIR SYSTEM COMMAND (AIR-520318), Washington, DC 20360

I. Machlin

NAVAL UNDERSEA RESEARCH AND DEVELOPMENT CENTER, Technical Library, Code 133, San Diego, CA 92132

Commander

NAVY FACILITIES ENGINEERING COMMAND, Department of the Navy, Code 042, Washington, DC 20390

M. D. Starr

NAVY SPACE SYSTEMS ACTIVITY, Air Force Unit Post Office, Los Angeles, CA 90045 ATTN: R. V. Silverman, Code 40

Commanding Officer

PACIFIC NORTHWEST LABORATORY, P.O. Box 550, Richland, WA 99352

Director

SANDIA CORPORATION, P.O. Box 5800, Albuquerque, NM 77115

J. R. Holland
J. McDonald

TRW SYSTEMS, One Space Park, Redondo Beach, CA 90278

J. Blumenthal
A. Hoffman
J. Ogren

WESTINGHOUSE ASTRONUCLEAR LABORATORY, P.O. Box 10864, Pittsburgh, PA 15231
William Buckman

USAEC OAK RIDGE OPERATIONS, P.O. Box E, Oak Ridge, TN 37830
Research and Technical Support

USAEC TECHNICAL INFORMATION CENTER, P.O. Box 62, Oak Ridge, TN 37830
(2)

☆U.S. GOVERNMENT PRINTING OFFICE: 1973-747-302/77